

## Origin of the high energy proton component below the geomagnetic cutoff in near earth orbit

L. Derome, M. Buénerd, A. Barrau, A. Bouchet, A. Menchaca-Rocha <sup>1</sup>, and T. Thuillier

*Institut des Sciences Nucléaires, IN2P3, 53 av. des Martyrs, 38026 Grenoble cedex, France*

Abstract: The high flux proton component observed by AMS below the geomagnetic cutoff can be well accounted for by assuming these particles to be secondaries originating from the interaction of cosmic ray protons with the atmosphere. Simulation results are reported.

The existence of a high flux proton component below the earth geomagnetic cutoff (GC), was reported recently by the AMS collaboration [1]. The observed spectrum has an intensity about equal to the cosmic primary proton flux above GC. It has a maximum at low momenta and extends from the momentum threshold of the spectrometer at  $\approx 0.4$  GeV/c, up to the GC around 10 GeV/c in the equatorial region, where the high momentum tail merges with the primary proton spectrum above GC.

It has been demonstrated long ago that such subGC component cannot be part of the primary proton flux [2, 3]. It has to be a secondary product of the primary cosmic ray (CR) flux on earth. This note reports on an attempt both to identify which part of the incident CR flux on earth generates this spectrum and by which mechanism, and to investigate its dynamical status with respect to the trapping process observed for other circum-terrestrial populations of particles.

A similar phenomenon was observed previously with the very high intensity low energy proton flux measured in the Van Allen belts, at kinetic energies typically below 100 MeV and for distances typically beyond 1.2 earth radius, which was interpreted as originating from secondary neutrons produced on atmospheric nuclei by CR protons [4]. Many low energy neutrons are produced by nuclear evaporation, or spallation, or preequilibrium nuclear emission, which can constitute the source term driving the equilibrium of this population.

The situation is quite different for the population of higher momentum protons, beyond 0.5 GeV/c, observed here. It is too high in energy to be accounted for by the above quoted mechanism, neither could it be by neutrons from the direct charge exchange reaction  $pn \rightarrow np$ , induced by high energy CR protons of nuclei, because of highly unfavored kinematics and small cross sections of the diffractive production mechanism, and very small probability of neutron decay below the altitude of AMS.

The two most significant sources of secondary protons over the observed energy range are the  $p+\mathcal{A}$  and  ${}^4\text{He}+\mathcal{A}$  collisions,  $\mathcal{A}$  standing for atmospheric nuclei, the CR flux of higher nuclear masses being too small to contribute significantly.

Considering primary protons as a likely dominant source of the observed subGC protons, two extreme situations are met over the explored range of latitudes: In the equatorial region, primary and secondary spectra do not overlap, incident protons are above GC, then with  $E \geq 10$  GeV, and produce a spectrum of secondaries (below GC) with  $E \leq 10$  GeV, whereas in the polar region (no GSC) primary and secondary protons are totally mixed in a spectrum extending down to the 0.1 GeV kinetic energy

---

<sup>1</sup>Permanent address: Instituto de Física, IFUNAM, Mexico

range. This latter feature implies that a variety of reaction mechanisms, from nuclear in the low energy range to subnucleonic hadronic in the upper range, could contribute to generate the observed subGC population.

Experimentally, the  $pA \rightarrow pX$  reaction on light nuclei has been studied in several experiments over a broad range of incident energies [5, 6, 7, 8, 9, 10], (see [12, 13] for inclusive  $pp \rightarrow pX$  studies) providing a body of data rich enough for systematic trends to be identified and for a consistent physical picture of the dominant mechanisms to emerge. Two components were observed in the measured proton spectra, which could be qualitatively identified to two different regimes of collision. One is forward peaked, dominated with leading particle effects, and corresponds to peripheral collisions and low orders of multiple intranuclear proton-nucleon collisions. The closeness of the experimental forward proton multiplicities measured in  $pA$  [14] and  $pp$  [13] collisions support this picture and shows in addition that protons measured in the first reaction are dominantly hadronic products of  $pp$  collisions. This is also consistent with the known proton mean free path in nuclei [15]. The other component corresponds to more central collisions and higher order type of multiple intranuclear collisions. In the following, these two components will be referred to as *quasi elastic* (QE) and *deep inelastic* (DI) respectively, following ref [8]. In ref [8], the first component was observed for low energy protons only in the angular range allowed by quasi free scattering kinematics, whereas the other component was observed also at backward angles in the region of zero rapidity, kinematically not accessible to free proton-nucleon processes. The two components have been found to exhibit significantly different dependence on the nuclear target mass, supporting the above description [7, 8].

In this context, the following features of the reactions relevant to the present study, have been observed: a) The invariant cross section for proton production versus transverse kinetic energy, can be described with a simple exponential over the transverse mass, with a slope weakly dependent on the rapidity [10]. b) At backward angles, a limiting production mechanism has been observed for incident energies above 8.5 GeV/c [6, 8, 9], the cross-section showing little incident energy dependence, with the onset of the limiting behaviour occurring as low as 1-2 GeV kinetic energy per nucleon for protons produced within the range 0.4-1 GeV/c [7]. It was shown in ref [8] that the target-like proton production can be described with a simple parametrization over the full angular range (see ref [11] and the quoted refs in this paper for the theoretical aspects).

The inclusive spectrum of protons at the altitude of AMS (390-400km) has been calculated by means of a computer simulation program built to this purpose. CR particles are generated with their natural abundance and momentum distributions [16] corrected for the solar modulation effect [17], at a distance of 5 terrestrial radii, or 2 Störmer length units [2] in order to ensure the generation point to be always in appropriate initial conditions for the earth magnetic field. They are propagated inside the earth magnetic field [18], using 4th order adaptative Runge-Kutta integration of the equation of motion. Particles are allowed to interact with atmospheric nuclei (mainly  $^{14}\text{N}$  and  $^{16}\text{O}$ , see ref [19] for the model of atmosphere) and produce secondary protons with cross sections and multiplicities as discussed below. Each secondary proton is then propagated and allowed to collide as in the previous step. A reaction cascade can thus develop through the atmosphere. The reaction products are counted when they cross the virtual sphere at the altitude of the AMS spectrometer, upward and downward. Particles undergo energy loss by ionisation before and after the interaction. Multiple scattering effects have not been included at this stage. Each event is propagated until the particle disappears by either colliding with a nucleus, or being stopped in the atmosphere, or escaping to outer space beyond twice the production altitude. A 2000 s time out protection in the program has never been called for the simulated sample. It must be noted that particles are counted each time they cross the sphere of detection altitude. The contributions of trapped particles are thus weighted statistically with their numbers of crossings, which increases in proportion their contribution to the final spectrum. Some empirical cuts over the initial particle kinematics allowed significant computer time saving by rejecting

kinematically irrelevant events.

The secondary nucleon spectrum generated has to cover two orders of magnitudes in kinetic energy, between about 100 MeV and 10 GeV. The main component of proton production cross section was obtained by means of analytical relations fitted to the 14.6 GeV  $p + Be$  data [10] using the slope parameters given in this reference for the transverse mass distribution, whereas the slowly varying rapidity distributions were fitted with a polynomial. The scaling properties have been checked with the FRITIOF/PYTHIA (Lünd) event generator [20]. Since this generator is not expected to account for the very low energy and backward proton emission (target-like to negative rapidities), this latter component was incorporated using of the parametrization given in ref [8]. The respective contributions to the total multiplicity-weighted proton production cross-section, were 352 mb for the QE component and 88 mb for the DI components. Cross sections on atmospheric nuclei were renormalized from the original data or parametrizations obtained on different nuclei, using ratios of geometrical cross sections. Figure 1 shows the two proton components as a dashed line (QE), and solid line (DI) from  $p + C$  at 7.5 GeV. For 125 MeV protons, it is seen that the data [8] are pretty well reproduced by the sum of the two components, providing sound grounds to the present calculations. For each event, the proton multiplicity was generated using a Poisson distribution with the experimental mean value  $\mu=1.7$  from ref [14]. Neutron spectra and multiplicities were taken identical to proton's.

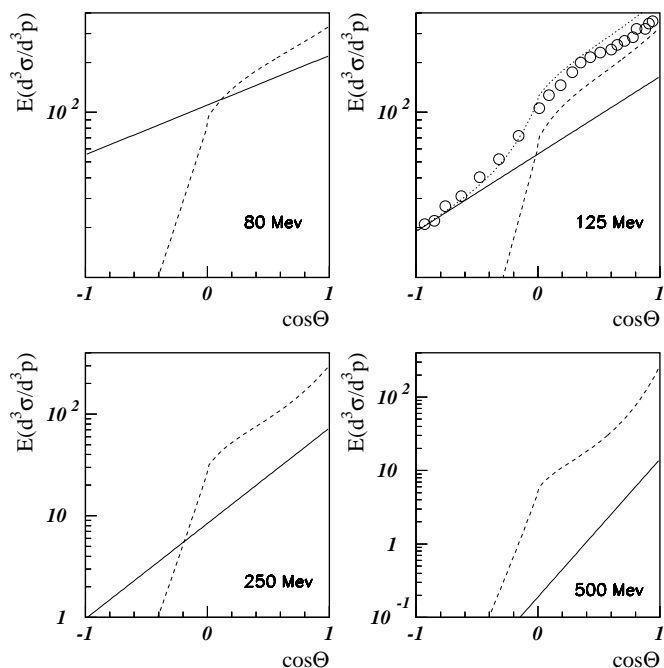


Figure 1: Angular distributions of the two proton components from  $pp$  collisions included in the simulation, for low secondary proton energies: Parametrization of ref [10] data (dashed line), and parametrization from ref [8] (solid line). In the upper right plot, the sum of the two components is compared to the data from [8].

A sample of  $6 \cdot 10^7$  particles was generated over the terrestrial sphere (120 hours of CPU computing time), of which  $2.7 \cdot 10^6$  reached the atmosphere, corresponding to a sampling time of the incident flux of the order of 0.5 ps. A cut requiring the accepted events to be inside the angular acceptance of AMS [1] was applied to the detected protons. Figure 2 shows some basic features of the simulated sample. The four histograms show respectively, the distribution of the altitude of the interaction points (upper left), the thickness of matter crossed by particles (upper right), the lifetime of particles

between production and detection (lower left), and the rank of the event in the atmospheric collision cascade (lower right). The distribution of the proton production altitude has a maximum around

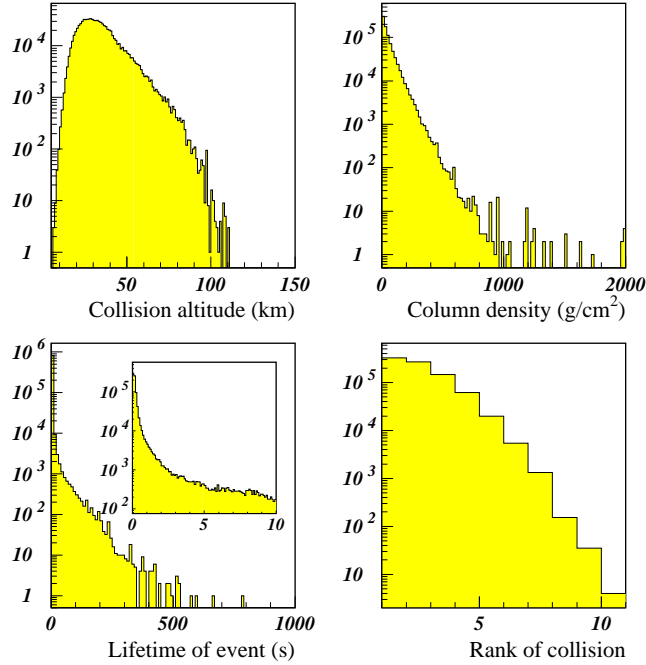


Figure 2: *Distributions of production altitude (km), thickness of matter crossed ( $\text{g}/\text{cm}^2$ ), propagation time (s) between particle production and detection, and distribution of the rank of the collision in the atmospheric cascade for a given event, for the simulated sample of events.*

25 km (mean value 39 km), and then decays approximately exponentially, following the atmospheric density profile. The thickness of matter crossed by the particles is distributed over a range extending up to about  $600 \text{ g}/\text{cm}^2$ , i.e., about 10 collision lengths, as it could be expected from the known range of the incident particles. The lifetime of the particles extends up to around 600 s. The insert shows the distribution between 0 and 10 s. The lifetime vs momentum correlation obtained (not shown) is in qualitative agreement with the backtracing calculations reported in [1].

It is seen on the lower right histogram that more than 50% of the detected protons are not produced in the first collision, and originate from up to the 10th collision generation in the atmospheric cascade for a given incident proton. An expected correlation is observed between collision rank and production altitude.

Figure 3 displays an important feature of these results with the scatter plot of the detection latitude versus the number of crossings of the detection altitude. It shows that events with large crossing multiplicities are strongly correlated with low latitudes, thereby showing that a population of trapped particles confined in the equatorial region  $\approx \pm 0.3 \text{ rad}$  is expected to be observed experimentally.

In addition, the following other features are observed:

- A population of longlived particles, with flight times up to several  $10^2 \text{ s}$ , is found in the polar region, more than 95% of them having only one or two crossings, i.e., having very long flight path between two crossings. The energy distribution of these particles is the same as that of particles at lower latitudes. Their trajectories then make large loops away from earth.
- The angular distribution of the detected protons with respect to the incident proton direction, resulting from the folding of the (forward peaked) cross section of the proton production reaction

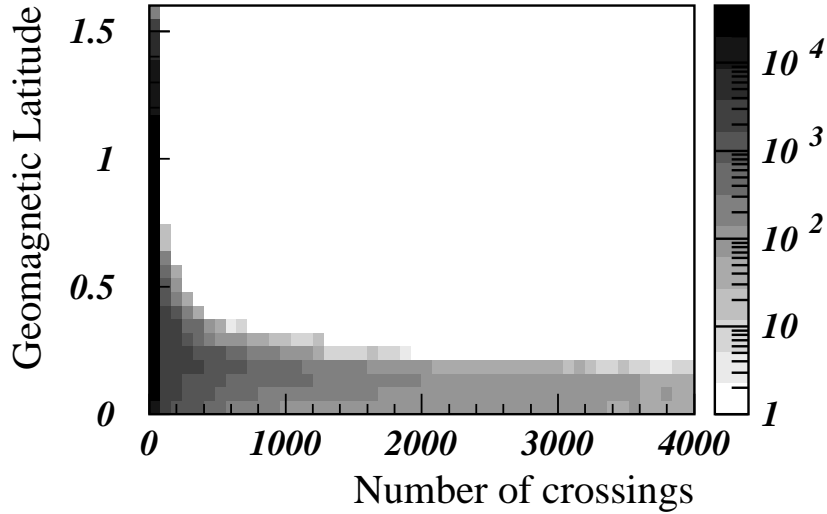


Figure 3: Two dimensional plot of the distribution of the CGR (geomagnetic) latitude [21] versus number of crossings of the detection altitude, showing that a population of particles is trapped in the equatorial region.

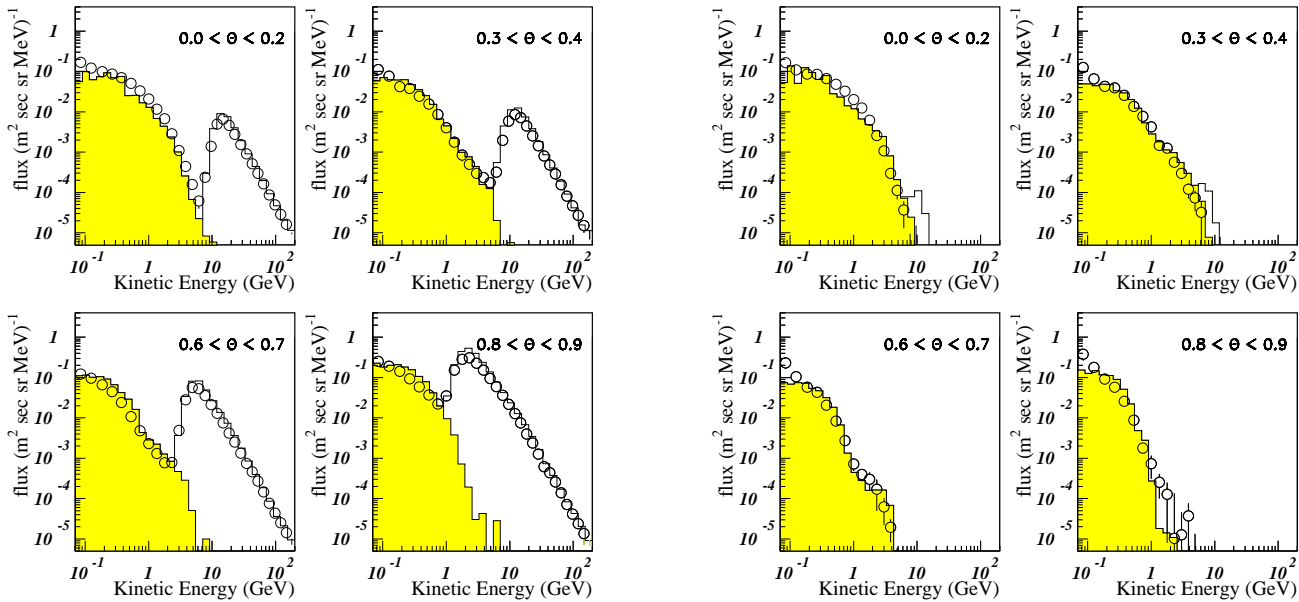


Figure 4: Experimental kinetic energy distributions from [1] for a sample of bins in latitudes (open circles), compared to the results of the simulation (full line) described in the text, for downward (left) and upward protons.

with the (outward peaked) momentum acceptance of the magnetospheric transport system, is found to be approximately evenly distributed over the forward hemisphere and decaying rapidly at backward angles.

Figure 4 shows the experimental kinetic energy distributions of downward (left) and upward (right) protons measured for some bins of latitude, compared to the results of the simulation. No free parameter is used for normalization to the data: The calculated results are entirely determined by the physics input to the calculation. It is seen that the agreement between the data and the simulation result is remarkably good, at all latitudes and for both the inward and outward flux. In particular, the cutoff region is particularly well reproduced, which indicates that the processing of the particle dynamics and kinematics is good. The shaded histograms in the figure correspond to secondary particles in the simulation. The fraction of events originating from the DI component of the proton production cross section described previously, vary from about 10% in the equatorial region up to 25% in the polar region, with a momentum distribution peaking at low kinetic energy and distributed below 500 MeV.

It must also be noted that the broad enhancement observed experimentally in the 1 GeV region in the subGC spectrum for the equatorial latitude compared to the other latitudes, is quite well reproduced. It has been verified that this enhancement is mainly due to the population of trapped particles above 10 crossings as shown on figure 3. The energy distribution of this population is confined below about 3 GeV since particles circling vertically in the earth magnetic field around the mean AMS altitude (380 km) have a Larmor radius of approximately 110 km per GeV/c.

The calculated flux at very low momenta shows a more or less significant deficit compared to the data for most latitudes. Since more than 50% of the detected particles originate from secondary nucleon interaction with the atmosphere, the concerned incident energy range extends down to values where contributions of nuclear processes not taken into account by the event generator, could account for the observed deficit. A defect of the particle trapping processing at low momenta is also possible however.

The  $^4\text{He}$  cosmic flux should also contribute to the studied population. This contribution should roughly scale with the ratio of incoming flux of  $^4\text{He}$  and protons, since after the primary interaction, the atmospheric cascade should develop the same way. It is therefore expected to be about one order of magnitude smaller than the cosmic proton contribution [16], which would not change significantly the results. Detailed investigations are in progress on the above points.

The AMS measurements constitute a new input to the calculations of atmospheric neutrino production (see refs [22] for example). New calculations are clearly required to evaluate the effect of the observed subGC component of the proton flux on the neutrino flux. It must be observed that the two proton populations, above and below GC, do not have the same interaction probability and angular distribution, and then will not affect equally the atmospheric neutrino flux.

In summary it has been shown that the high intensity flux of protons observed below the geomagnetic cutoff by the AMS experiment can be well reproduced by assuming that this flux originates from the interaction of the primary proton Cosmic Ray flux with the atmosphere. The technical means developed in this work are being applied to the investigation of the other particle populations observed by AMS. They are also potentially useful for similar calculations concerning other experiments such as the atmospheric antiproton component in satellite and balloon experiments, as well as for many other related processes and particle populations. Detailed results will be reported in a more comprehensive paper in preparation.

## References

- [1] J. Alcaraz et al., Phys. Lett. B472(2000)215

- [2] C. Störmer, *The Polar Aurora*, Clarendon Press (Cambridge), 1955; See also M.S. Vallarta, *Handbuch der Physik*, Springer Verlag, Vol 61/1, p 88, 1961.
- [3] S.F. Singer and A.M. Lenchek, *Prog. in Elem. Part. and Cosm. Ray Phys.* Vol 6, p 245, NHPC, 1962.
- [4] E.C. Ray, *J. Geophys. Res.*, 65(1960)1125
- [5] W.F. Baker et al., *Phys. Rev. Lett.* 7(1961)101; V.L. Fitch, S.J. Meyer, and P.A. Pirou, *Phys. Rev.* 126(1962)1849; R.A. Lundy et al., *Phys. Rev. Lett.* 15(1965)504; J.V. Allaby et al., CERN report 70-12 (1970); T. Eichten et al., *Nucl. Phys.* B44(1972)333; K. Nakai, *Perspective in Meson Science*, Edited by T. Yamazaki, K. Nakai, and K. Nagamine, NHPC, 1992, p 685.
- [6] Y.D. Bayukov et al., *Phys. Rev.* C20(1979)764
- [7] J.V. Geaga et al., *Phys. Rev. Lett.* 45(1980)1993
- [8] Y.D. Bayukov et al., *Sov. J. of Nuc. Phys.* 42(1985)116
- [9] S.V. Boyanov et al., *Sov. J. of Nuc. Phys.* 46(1987)871
- [10] T. Abbott et al., *Phys. Rev.* D45(1992)3906
- [11] P. Danielewicz, *Phys. Rev.* C42(1990)1564
- [12] D. Dekkers et al., *Phys. Rev.* 137(1962)B962; E.W. Anderson et al., *Phys. Rev. Lett.* 19(1967)198; E.W. Anderson and G.B. Collins, *Phys. Rev. Lett.* 19(1967)201; G.J. Marmer et al., *Phys. Rev. Lett.* 23(1969)1469; U. Amaldi et al, *Nucl. Phys.* B86(1975)403
- [13] A.M. Rossi et al, *Nucl. Phys.* B84(1975)269;
- [14] A. V. Aref'ev et al., *Sov. J. of Nuc. Phys.* 28(1978)789
- [15] I. Tanihata, S. Nagamiya, S. Schnetzer, and H. Steiner, *Phys. Lett.* B100(1981)121
- [16] J.A. Simpson, *Ann. Rev. Nucl. and Part. Sci.* 33(1983)323; B. Wiebel-Sooth, P.L. Biermann, and H. Meyer, *A&A*, 330(1997)389
- [17] J.S. Perko, *Astro. Astrophys.* 184(1984)119; see M.S. Potgieter, *Proc. ICRC Calgary*, 1993, p213, for a recent review of the subject.
- [18] N.A. Tsyganenko, *J. Geophys. Res.* 100(1995)5599; N.A. Tsyganenko and D.P. Stern, 101(1996)27187
- [19] A.E. Hedin, *J. Geophys. Res.* 96(1991)1159
- [20] Hong Pi, *Comput. Phys. Commun.* 71(1992)173
- [21] G. Gustafsson, N.E. Papitashvili, and V.O. Papitashvili, *J. Atmos. Terr. Phys.* 54(1992)1609; See also A. Brekke, *Physics of the Upper Polar Atmosphere*, pp 127-145, Wiley and Sons Eds, 1997.
- [22] T.K. Gaisser, *Nucl. Phys. Proc. Suppl.* 87(2000)145; R. Engel and T.K. Gaisser, *Phys. Lett.* B472(2000)113